Geoderma 467 (2026) 117746

Contents lists available at ScienceDirect

Geoderma

journal homepage: www.elsevier.com/locate/geoderma

Changes in natural ^{15}N abundance highlight warming-induced stimulation of soil nitrate losses by coupled nitrification–denitrification in an old-growth montane forest

Michaela Bachmann [a,b,*,1], Ye Tian [a,c], Jakob Heinzle [d], Werner Borken [e], Erich Inselsbacher [f], Wolfgang Wanek [a,*,1], Andreas Schindlbacher [d]

[a] Division of Terrestrial Ecosystem Research, Department of Microbiology and Ecosystem Science, Center of Microbiology and Environmental Systems Science, University of Vienna, Djerassiplatz 1, A-1030 Vienna, Austria
[b] Systemic Risk and Resilience Research Group, International Institute for Applied Systems Analysis, Schlossplatz 1, 2361 Laxenburg, Austria
[c] Department of Soil and Environment, Swedish University of Agricultural Sciences (SLU), Lennart Hjelms Väg 9, 75007 Uppsala, Sweden
[d] Department of Forest Ecology and Soil, Federal Research and Training Centre for Forests, Natural Hazards and Landscape-BFW, Seckendorff-Gudent Weg 8, 1131 Vienna, Austria
[e] Department of Soil Ecology, Bayreuth Center of Ecology and Environmental Research (BAYCEER), University of Bayreuth, Dr. Hans-Frisch-Straße 1-3, 95448 Bayreuth, Germany
[f] BOKU University, Department of Ecosystem Management, Climate and Biodiversity, Institute of Soil Science, Peter-Jordan-Straße 82, 1190 Wien, Austria

ARTICLE INFO

Handling Editor: Jan Willem Van Groenigen

Keywords:
Climate change
Long-term warming
soil N cycle
Nitrification
Denitrification
^{15}N isotope

ABSTRACT

Climate warming alters biogeochemical cycles, especially in high-altitude forests where warming accelerates soil organic matter decomposition and CO_2 efflux. Faster nitrogen (N) mineralization can enhance N availability to plants but may also increase N losses if soil microbial N use efficiency declines. However, long-term data on soil N loss mechanisms remain scarce. Key N cycling processes affect the natural ^{15}N:^{14}N isotope ratio ($\delta^{15}N$) differentially, with (de)nitrification yielding ^{15}N-depleted products and leaving residual pools ^{15}N-enriched. We investigated belowground N cycling after 14 years of soil warming (+4 °C) in a temperate old-growth forest in Achenkirch, Austria, by measuring $\delta^{15}N$ values in belowground N pools (root N, bulk soil N, microbial biomass N, ammonium, nitrate) through isotope ratio mass spectrometry. Warming had no effect on $\delta^{15}N$ of bulk soil N, microbial biomass N, and nitrate, but significantly increased $\delta^{15}N$ in root N (−5.0 to −4.1‰) and in soil ammonium (−2.9 to 1.1‰). Root $\delta^{15}N$, reflecting inorganic soil N, indicates that warming-induced N losses caused ^{15}N enrichment of inorganic soil N. Elevated ammonium $\delta^{15}N$ points to increased rates of nitrification, while nitrate $\delta^{15}N$ patterns imply denitrification (60–65% of nitrate sink) exceeding leaching as the main loss pathway, which aligns with available field observations. Coupled plant–soil $\delta^{15}N$ analysis thus revealed decadal warming-driven changes in N cycling and identified coupled nitrification–denitrification as a key pathway of soil N loss, which is otherwise difficult to measure directly.

1. Introduction

Climate warming is expected to have a lasting impact on global forest ecosystems, influencing tree growth, shifting tree species distributions, increasing disturbance events such as wildfires and insect outbreaks, and affecting the resilience and productivity of forest ecosystems (Nolan et al. 2018; Yuan et al. 2018; Canadell et al. 2021). Moreover, global warming affects biogeochemical processes such as soil carbon (C) and nitrogen (N) cycling (Sun et al. 2022; Mao et al., 2025b), stimulating mineralization and nitrification (Butler et al. 2012; Salazar et al. 2020)

Abbreviations: C, Carbon; CFE, Chloroform Fumigation Extraction; Δ, Isotope Fractionation; δ, Isotope Deviation; MAP, Mean Annual Precipitation; MAT, Mean Annual Temperature; MBN, Microbial Biomass Nitrogen; N, Nitrogen; N_2, Dinitrogen; NO, Nitric Oxide; N_2O, Nitrous Oxide; NH_4^+, Ammonium; NO_3^-, Nitrate; NUE, Nitrogen Use Efficiency; PT-IRMS, Purge-and-trap Isotope-Ratio Mass Spectrometry; SOC, Soil Organic Carbon; SON, Soil Organic Nitrogen; TEN, Total Extractable Nitrogen.

* Corresponding authors at: Division of Terrestrial Ecosystem Research, Department of Microbiology and Ecosystem Science, Center of Microbiology and Environmental Systems Science, University of Vienna, Djerassiplatz 1, A-1030 Vienna, Austria (M. Bachmann).

[1] Shared co-authorship.

https://doi.org/10.1016/j.geoderma.2026.117746
Received 27 October 2025; Received in revised form 29 January 2026; Accepted 19 February 2026
Available online 21 February 2026
0016-7061/© 2026 The Authors. Published by Elsevier B.V. This is an open access article under the CC BY-NC-ND license (http://creativecommons.org/licenses/by-nc-nd/4.0/).

as well as plant N uptake (Hu et al. 2024; Wang 2024). An acceleration of soil N cycling can be accompanied by ecosystem N retention if microbial nitrogen use efficiency (NUE) and/or plant uptake are high. Microbial NUE depicts how much soil organic N acquired by soil microbes is retained in their biomass and allocated to microbial growth, with the excess being deaminated and excreted as ammonium (NH_4^+) through N mineralization processes. Therefore, if microbial NUE declines and organic N mineralization and nitrification increase, soil N losses are likely to rise through hydrological and gaseous pathways. However, the literature reports mixed responses of soil N loss processes to climate warming (Bai et al. 2013; Sun et al. 2022; Mao et al. 2025b), with reported increases, decreases, or negligible changes. The variable responses depend on whether warming primarily enhances N mineralization and nitrification (increasing nitrate (NO_3^-) availability and leaching risk) or instead strengthens plant and microbial N retention and immobilization. Moreover, warming effects differ across moisture regimes and ecosystem types, because interactions with soil water balance and redox conditions can shift the dominant loss pathway between leaching and gaseous emissions (Mao et al. 2025b). Finally, continuous forest soil warming is often associated with concomitant declines in soil moisture content (Xu et al. 2013), thereby triggering combined ecosystem warming–drying responses.

Long-term soil warming experiments have provided important insights into how elevated temperatures alter individual components of the soil N cycle, including enhanced extracellular enzyme activities, accelerated organic matter decomposition, and increased gross N mineralization (Bai et al. 2013; Meng et al. 2020; Mao et al. 2025b). At the Achenkirch warming experiment, previous studies have demonstrated increased activities of enzymes targeting macromolecular N and a decline in NUE, indicating a shift toward faster N turnover and a greater potential for N loss (Tian et al. 2023a). At the same time, direct measurements of soil N losses have yielded ambiguous results: soil N fluxes via molecular diffusion mechanisms showed no consistent warming response (Heinzle et al. 2021), warming effects on N_2O emissions were transient, and high spatial heterogeneity of N_2 emissions from denitrification limited the detectability of treatment effects (Heinzle et al. 2023). Despite concurrent declines in soil organic carbon and total soil N stocks under warming (Tian et al. 2023a), the dominant pathways and integration of soil N losses over time therefore remain unresolved.

This apparent mismatch between enhanced internal N cycling and equivocal flux-based evidence for N losses highlights a key limitation of process-specific measurements: individual fluxes are often episodic, spatially variable, and temporally decoupled from longer-term changes in ecosystem N pools. In this context, natural-abundance stable nitrogen isotope ratios ($\delta^{15}N$) offer a complementary and integrative approach to assess ecosystem-scale N dynamics under warming. Because most biologically mediated N transformations — including organic N depolymerization, NH_4^+ oxidation, denitrification, and inorganic N assimilation — discriminate against the heavier isotope (^{15}N), preferential losses of isotopically light N through gaseous or hydrological pathways lead to progressive ^{15}N enrichment of residual soil and plant N pools (Mariotti et al. 1981; Handley & Raven 1992; Denk et al. 2017). In contrast, physical transport processes alone exert negligible isotope effects.

$\delta^{15}N$ approaches integrate the cumulative imprint of multiple N loss pathways over time and can reveal changes in the openness of the soil N cycle even when individual loss fluxes are difficult to detect directly. Importantly, contrasting isotope fractionation signatures associated with nitrification–leaching versus denitrification-driven gaseous losses provide a basis for distinguishing dominant N loss pathways at the ecosystem level. Previous studies have successfully applied a simplified isotope framework to infer warming-induced changes in N losses and N-cycle openness (Liao et al., 2021), the direction of $\delta^{15}N$ change differing by ecosystem, soil pH, climate and mechanism. Increased N cycle openness was, for instance, highlighted by ^{15}N enrichment of vegetation under elevated temperatures in subalpine woody vegetation (Dawes et al. 2017). However, more mechanistic frameworks to identify changes in loss pathways upon warming have not yet been applied.

In this study, we applied a natural-abundance $\delta^{15}N$ model based partitioning approach to assess long-term warming effects (14-year period) on ecosystem N cycling at the Achenkirch experimental facility, a soil warming experiment in a montane old-growth forest in Tyrol, Austria. We quantified $\delta^{15}N$ of bulk soil N, microbial biomass N, fine root N, and inorganic N pools (NH_4^+ and NO_3^-) across three seasons (spring, summer, and autumn) to evaluate the consistency of warming effects and to infer dominant soil N loss pathways. By integrating isotopic evidence with existing knowledge of warming-induced changes in enzyme activity, microbial NUE, and gaseous N fluxes, our approach provides a necessary ecosystem-scale perspective on how long-term warming alters the balance between N retention and loss.

By analyzing soil ^{15}N abundances, we therefore expected that (i) increased SOM decomposition and lower microbial NUE would cause mineralization and nitrification to increase, which should be reflected in elevated soil $\delta^{15}N_{NH4+}$ in warmed plots. We further hypothesized that (ii) under ambient conditions (high precipitation and moist, high soil organic carbon soils), denitrification substantially contributes to soil NO_3^- loss and enriches residual NO_3^- in ^{15}N, whereas warming reduces soil moisture and denitrification, resulting in lower ^{15}N enrichment of NO_3^- relative to NH_4^+ in warmed compared with control soils.

2. Material and methods

2.1. Site description

The experimental site is located in Achenkirch, Tyrol, Austria (47°34050"N; 11°38021"E), at 910 m a.s.L. in the Northern Alps. Climatic conditions are cool and humid with mean annual temperature (MAT) of 7.0 °C and mean annual precipitation (MAP) of 1493 mm (mean 1988–2017, data supplied by GeoSphere Austria). The site is usually snow covered from November/December until April/May. The forest is approximately 130 years old, situated on dolomite bedrock and dominated by *Picea abies* (~80%), with interspersed *Fagus sylvatica* and *Abies alba*. The forest soil is characterized as shallow Chromic Cambisol and Rendzic Leptosol (IUSS Working Group WRB 2022). Soil warming plots were established in 2004 (n = 3) and in 2007 (n = 3), currently comprising six paired warmed and control plots (resulting in 12 subplots), each measuring 2 x 2 m. The heated subplots are equipped with resistance heating cables (0.4 cm diameter) installed at a depth of 3 cm, with 7–8 cm spacing between cables, warming the soil by + 4 °C above ambient temperature of the paired control subplot during snow-free season (Schindlbacher et al. 2015). Warming is inactive during periods of snow cover.

2.2. Sampling and measurements

Soil samples were collected in May, August, and October 2019. In each subplot, 5–8 subsamples were taken from 0-10 cm soil depth with a 2.5 cm diameter corer and mixed into a single composite sample per subplot, which yielded 36 soil samples in total. After sieving through 2 mm mesh and removing stones, fine roots were picked, washed, dried at 60 °C, and weighed. Aliquots of fresh soil (~4 g) were weighed in for (i) determination of soil water content and soil total N, (ii) chloroform fumigation extraction (CFE) for microbial biomass N (MBN) determination, and (iii) direct extraction of NH_4^+ and NO_3^- (as well as total extractable N, TEN). For gravimetric determination of soil water content, soil samples were dried in a drying oven (105 °C) and dry mass measured. To determine MBN, soils were fumigated with chloroform in a desiccator for 48 h. Fumigated and untreated soil samples were then extracted with 0.5 M K_2SO_4 (1:7.5 (w:v)), filtered through ash-free cellulose filters, and the extracts stored at −20 °C.

K_2SO_4 extracts from non-chloroform treated soils were analyzed colorimetrically for NH_4^+ and NO_3^- concentrations (Hood-Nowotny et al.,

2010). TEN was quantified using a TOC/TN-Analyzer (TOC-VCPH/CPNT-NM-1, Shimadzu, Japan) in K_2SO_4 extracts from chloroform fumigated and untreated soils. MBN content (Jenkinson et al., 2004) was calculated as follows:

$$MBN = (TEN_{fumigated} - TEN_{non-fumigated})/K_{EN}$$

where $TEN_{fumigated}$ and $TEN_{non\text{-}fumigated}$ are TEN concentrations in the fumigated and the non-fumigated soils, respectively, and K_{EN} is the correction factor of 0.45 for MBN estimation.

The total N contents and the N isotopic composition of fine roots and of bulk soils were measured by elemental analyzer-isotope ratio mass spectrometry (EA-IRMS), consisting of an EA-Isolink coupled via a ConFlo IV interface to a Delta V Advantage IRMS (Thermo Scientific, Bremen, Germany). Dried samples were finely ground in a ball mill (Retsch MM200, Hainau, Germany) and weighed into tin capsules before analysis by EA-IRMS.

The N isotopic composition of labile soil N pools (TEN, MBN, NH_4^+ and NO_3^-) was measured after conversion to N_2O by purge-and-trap isotope-ratio mass spectrometry (PT-IRMS). The PT-IRMS system consisted of a Gasbench II headspace gas analyzer with an integrated cryotrap for N_2O pre-concentration, coupled to a Delta V Advantage IRMS (Thermo Scientific, Bremen, Germany).

The isotopic composition of three operationally defined nitrate pools was determined: (i) soil native NO_3^-, (ii) TEN-derived NO_3^-, and (iii) MBN-derived NO_3^-. Soil native NO_3^- refers to nitrate present in soil extracts prior to any chemical oxidation and was analyzed directly. TEN-derived NO_3^- represents nitrate produced by alkaline persulfate oxidation of total extractable nitrogen (TEN), thereby converting all extractable organic N and NH_4^+ quantitatively to NO_3^- prior to isotope analysis. MBN-derived NO_3^- represents nitrate derived from microbial biomass N and was calculated as the difference in TEN-derived NO_3^- between fumigated and non-fumigated soil extracts following chloroform fumigation. For isotope analysis, NO_3^- from all three pools was converted to N_2O using the VCl_3–azide method (Lachouani et al. 2010). Alkaline persulfate digestion was applied to extracts from both non-fumigated and fumigated soils prior to isotope analysis of TEN-derived and MBN-derived NO_3^-, whereas soil native NO_3^- was analyzed without prior oxidation. To prepare the persulfate reagent, 44.04 g $Na_2S_2O_8$, 16.8 g NaOH, and 30 g H_3BO_3 were dissolved in 1 L deionized water. An amino acid and a $NO3^-$ standard series (1:2 dilution from 500 μM − 3.9 μM) were prepared in 0.5 M K_2SO_4 to determine the digestion efficiency of organic N and to calibrate the method for concentration. Isotopic calibration was performed using five isotopically distinct amino acids (laboratory standards), pre-characterized before using EA-IRMS in our laboratory. Samples (samples and standards) and persulfate reagent were mixed in a 1:1 ratio in 1.5 mL HPLC glass vials and autoclaved for 60 min at 120 °C. The resultant NO_3^- from persulfate digestion as well as NO_3^- in the undigested K_2SO_4 extracts were converted to N_2O using the VCl_3-azide method. For this, NO_3^- in the respective samples was converted to N_2O in two steps: Vanadium (III) chloride (VCl_3) reduced the NO_3^- to NO_2^-, which was then further reduced to N_2O by acidic sodium azide (Lachouani et al. 2010). Aliquots (500 μL) of the respective samples and standards (TEN, MBN or undigested K_2SO_4 extract for NO_3^-) were pipetted into 12 mL exetainers, closed and purged with helium for 10 min. After this, 100 μL sodium azide buffer (1.3 g NaN_3 in 10 mL Milli-Q, mixed 1:1 with 10% acetic acid, flushed with helium for 1 h) was injected into the exetainers with a gas-tight syringe to avoid air bubbles. Subsequently, 500 μL VCl_3 solution (0.79 g VCl_3 in 100 mL 3.2% HCl) was added to the samples, mixed on a vortex, and incubated at 37 °C for 24 h. To stop the reaction, 150 μL 6 M NaOH was injected to neutralize the NaN_3. The produced N_2O was transferred to empty, *He* purged and evacuated exetainers to avoid clogging of the PT-IRMS needle.

The N isotopic composition of MBN ($\delta^{15}N_{MBN}$) was calculated using a two-source mixing model with weighted calculations of isotope values:

$$\delta^{15}N_{MBN} = \frac{TEN_{fumigated} x \delta^{15}N_{fumigated} - TEN_{non-fumigated} x \delta^{15}N_{non-fumigated}}{TEN_{fumigated} - TEN_{non-fumigated}}$$

, where $TEN_{fumigated}$ and $\delta^{15}N_{fumigated}$ as well as $TEN_{non\text{-}fumigated}$ and $\delta^{15}N_{non\text{-}fumigated}$ are the contents and isotope signatures of TEN of fumigated and non-fumigated soils, respectively.

$\delta^{15}N_{NH4+}$ signatures were determined through microdiffusion with acid traps at alkaline solution pH followed by the BrO^--azide method (Zhang et al. 2015). For microdiffusion, acid traps were made of Teflon tape enclosing a cellulose disc, on which 4 μL 2.5 M $KHSO_4$ was pipetted, before sealing them. Then, 0.1 g MgO was weighed in 20 mL scintillation vials, followed by 10 mL of the K_2SO_4 extracts. One acid trap was added to each vial. The vials were placed on a shaker at 37 °C for three days. After the incubation, acid traps were removed and transferred into 1.5 mL reaction tubes for drying in a desiccator with concentrated sulfuric acid for three days. The dry cellulose discs were then removed from the Teflon covers, and the trapped NH_4^+ dissolved in 1 mL Milli-Q on a shaker for 30 min. In the meantime, 1 mL K_2SO_4 blanks (0.5 M), NH_4^+ concentration standards (50 μM to 1.56 μM NH_4Cl), and NH_4^+ isotope standards (at 15 μM, including reference materials IAEA-N-1 and IAEA-N-2 and two laboratory standards to cover the natural ^{15}N abundance range commonly encountered) were prepared and transferred to 12 mL exetainers. The sample extracts were pre-diluted according to previously measured photometric NH_4^+ concentration data in order to reach a final NH_4^+ concentration of 20 μM after microdiffusion and re-dissolution of trapped NH_4^+ and also transferred into exetainers (1 mL). To oxidize NH_4^+ to NO_2^-, a hypobromite reagent (BrO^-) was prepared. For this, 0.2 mL stock solution (0.12 g sodium bromate and 1 g sodium bromide in 50 mL MQ) was diluted to 10 mL with MQ, acid activated by adding 0.6 mL 6 M HCl for 5 min, and the reaction quenched by amendment of 10 mL 10 M NaOH. Then, 0.1 mL of this hypobromite reagent was added to all exetainers as an oxidation catalyst. After 30 min 33 μL sodium arsenite solution (0.51 g $NaAsO_2$ in 10 mL Milli-Q) was added to quench the reaction. To further convert NO_2^- to N_2O, 0.15 mL NaN_3 (1.3 g NaN_3 in 10 mL Milli-Q, mixed 1:1 with 10% acetic acid, flushed with helium for 1 h) was injected into the closed exetainers with a gas-tight syringe. After 30 min, the reaction was stopped by addition of 0.15 mL 10 M NaOH. Again, the N_2O produced was transferred to a new, He flushed and evacuated set of exetainers to determine the isotopic ratios by PT-IRMS.

The final calculation of the isotopic composition of samples included blank correction and isotope correction using respective isotope calibrations, following Lachouani et al. (2010). Nitrogen in N_2O formed during the VCl_3-azide reaction derives 1:1 from azide and NO_3^- (or NO_2^-) and therefore needs to be externally calibrated for isotopes.

2.3. Isotope notation and isotope modeling

Natural ^{15}N abundances are presented in the delta (δ) notation as follows:

$$\delta^{15}N(‰) = [\frac{(15N_{sample}/14N_{sample})}{(15N_{standard}/14N_{standard}} - 1] \quad (1)$$

This ^{15}N:^{14}N deviation (δ) of the sample from the international standard is expressed in ‰ (per mille) (Högberg 1997). A more positive δ value therefore refers to an enrichment of the sample with ^{15}N, whereas a more negative δ value suggests the opposite (Dawson & Siegwolf, 2007). Changes in isotopic abundance can be presented as isotope fractionation (Δ) by comparing the δ value of a substrate (δ_s) relative to its product (δ_p).

$$\Delta = ((\delta_s - \delta_p)/(1 + \delta_p/1000)) \quad (2)$$

In (semi-)closed systems isotopic compositions of the residual substrate (δ_{RS}) and of the cumulative product (δ_{CP}) can be calculated following

the Rayleigh isotope fractionation equations, depending on the fraction f of substrate converted to product, the isotope fractionation of the process (Δ) and the isotopic composition of initial substrates (IS, δ_{input}):

$$\delta_{RS} = \delta_{input} - \Delta^{*}ln(1-f) \quad (3)$$

$$\delta_{CP} = \delta_{input} + \Delta\frac{(1-f)}{f}^{*}ln(1-f) \quad (4)$$

We used the isotope fractionation framework (Xu et al. 2021) to roughly estimate the contribution of denitrification (versus NO_3^- leaching) to soil NO_3^- losses. Using the measured isotope signature of soil NH_4^+ we first predicted the instantaneous isotopic composition of NO_3^- formed due to nitrification, applying an average $\Delta_{nitrification}$ of 29.6‰ (Denk et al. 2017). NO_3^- leaching would not alter the isotope composition of this predicted NO_3^-, i.e. expressing $\Delta_{leaching}$ of 0.0‰, while denitrification has been shown to cause strong isotope fractionation, with $\Delta_{denitrification}$ of 31.4‰ (Denk et al. 2017). Following this approach we reformulated Equation (3) for denitrification, with δ_{RS} being equivalent to residual NO_3^- measured in soil, δ_{input} being $\delta^{15}N$ of instantaneous NO_3^- produced by nitrifiers from NH_4^+ (calculated as soil $\delta^{15}N_{NH4+}$ minus $\Delta_{nitrification}$ = 29.6; Denk et al. 2017), and f the fraction of NO_3^- removed by denitrification (not by leaching).

Accordingly, Equation (3) was adapted to the following,

$$\delta^{15}N_{residualNO3-} = (\delta^{15}N_{NH4+} - \Delta_{nitrification}) - \Delta_{denitrification}{}^{*}ln(1-f) \quad (3^{*})$$

and then solved for ln(1-f) and for $f_{denitrification}$.

$$ln(1-f) = \frac{(\delta^{15}N_{NH4+} - 29.6) - \delta^{15}N_{residualNO3-}}{\Delta_{denitrification}} \quad (5)$$

and

$$f = 1 - exp(ln(1-f)) \quad (6)$$

We only used average seasonal and treatment mean data for these estimations as indications for differences in the dominance of NO_3^- loss pathways. We here note that such calculations come with uncertainties, due to lack of knowledge of the *in situ* isotope fractionation factors of nitrification and denitrification, which can differ markedly between systems, and for not accounting of other processes consuming NO_3^- such as plant NO_3^- uptake and dissimilatory NO_3^- reduction to NH_4^+ (DNRA).

2.4. Data evaluation and statistics

After outlier correction, testing for normality, and data transformation of $\delta^{15}N$ values and N concentrations, Linear Mixed Effects Regression (*lmer*) models of each pool were calculated in R to assess statistical significance of the main effects *treatment* and *season* as well as their interaction (Pinheiro et al. 2019; Kuznetsova et al. 2017; Bates et al. 2015; Barton 2020). Values were considered significant at $p < 0.05$. Results were visualized with *ggplot* (Wickham 2016).

3. Results

The contents of bulk N, root N, MBN, NH_4^+ and NO_3^- in dry mass were not significantly affected by the soil warming treatment. In contrast, seasonality had a strong effect on the concentration of fine root N ($p < 0.001$), MBN ($p < 0.001$) and soil NO_3^- ($p < 0.001$). No significant interaction of season and treatment was found, indicating that the warming effect was consistent (yet non-significant) across seasons (Fig. 1; Table 1). Root N declined with season, from May to October, while MBN peaked in the summer season, and soil NO_3^- accumulated during the growing season, with maxima reached in autumn.

Across the ecosystem pools studied (Fig. 2), $\delta^{15}N$ values in bulk soil N were the most constrained, with $\delta^{15}N$ values ranging between −0.8 and 0.8‰ and being close to the isotope composition of atmospheric N_2. Roots were strongly ^{15}N depleted relative to bulk soils, fine roots ranging between −6.1 and −3.0‰. In contrast, soil microbes were strongly ^{15}N enriched, with $\delta^{15}N$MBN values ranging from 2.5 to 18.0‰. Inorganic N forms also showed strong variability in isotopic composition, following seasonal and treatment effects. Soil $\delta^{15}N_{NH4+}$ varied between −10.0 and 12.5‰, and soil $\delta^{15}N_{NO3-}$ between −5.0 and 7.5‰.

According to the *lmer*-models, the $\delta^{15}N$ values of all measured pools, i.e. bulk soil N ($p = 0.0015$), root N ($p < 0.001$), MBN ($p < 0.001$), NH_4^+ ($p < 0.001$) and NO_3^- ($p < 0.001$), were strongly affected by season. $\delta^{15}N$

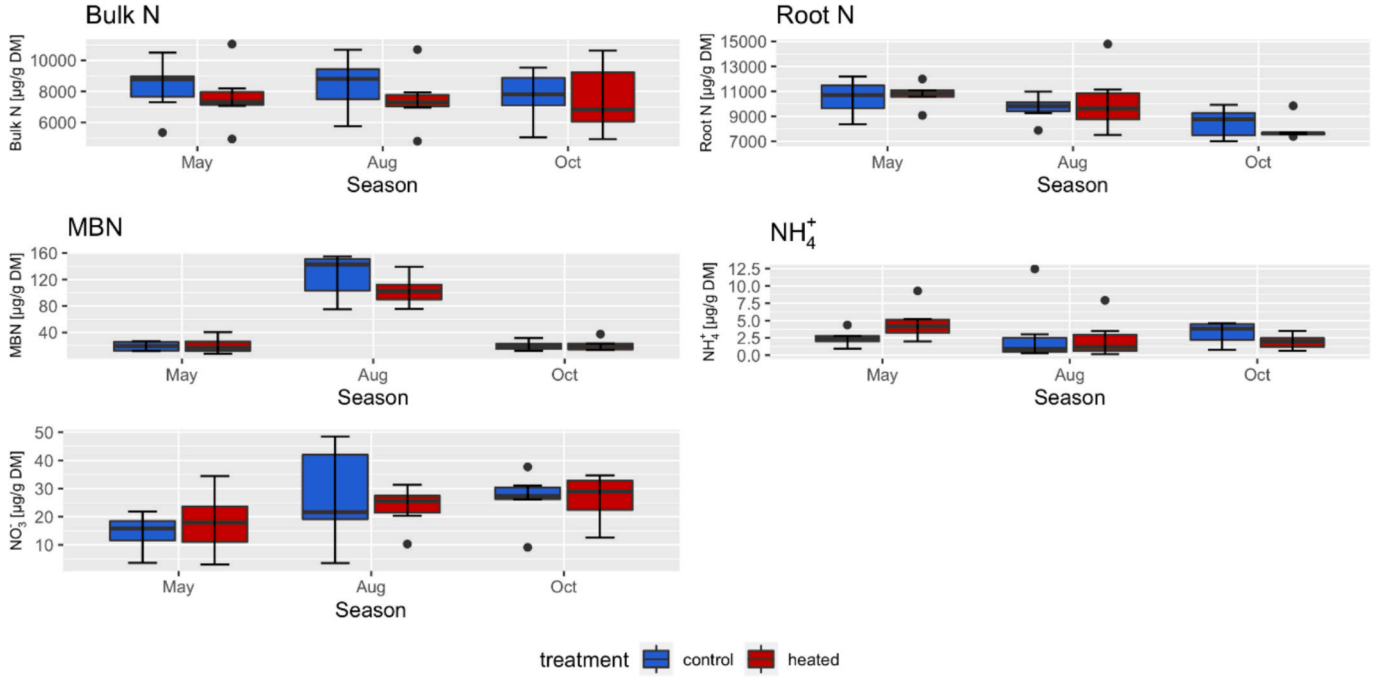

Fig. 1. Nitrogen contents of belowground N pools in warmed and control plots in the old-growth forest warming experiment in Achenkirch, Tyrol, Austria, during three sampling seasons. Contents are given in µg N/g DM for bulk N (soil total N), root N, MBN (soil microbial biomass N), NH_4^+ and NO_3^-.

Table 1
Summary of statistical significance of linear mixed effects models (lmer) and Kruskal-Wallis tests for N concentrations and $\delta^{15}N$ values in different belowground N pools. Transformation type is indicated where data were transformed to comply with variance homogeneity and normal distribution.

	Factor	Bulk N	Root N	MBN	NH_4^+	NO_3^-
Transformation		–	BoxCox	BoxCox	–	–
Concentration	Treatment	n.s.	n.s.	n.s.	n.s.	n.s.
	Season	n.s.	***	***	n.s.	*
	Interaction	–	n.s.	n.s.	–	–
Transformation		Squareroot	BoxCox	BoxCox	–	Log
$\delta^{15}N$ values	Treatment	n.s.	***	n.s.	**	n.s.
	Season	**	***	***	***	***
	Interaction	n.s.	n.s.	*	n.s.	n.s.

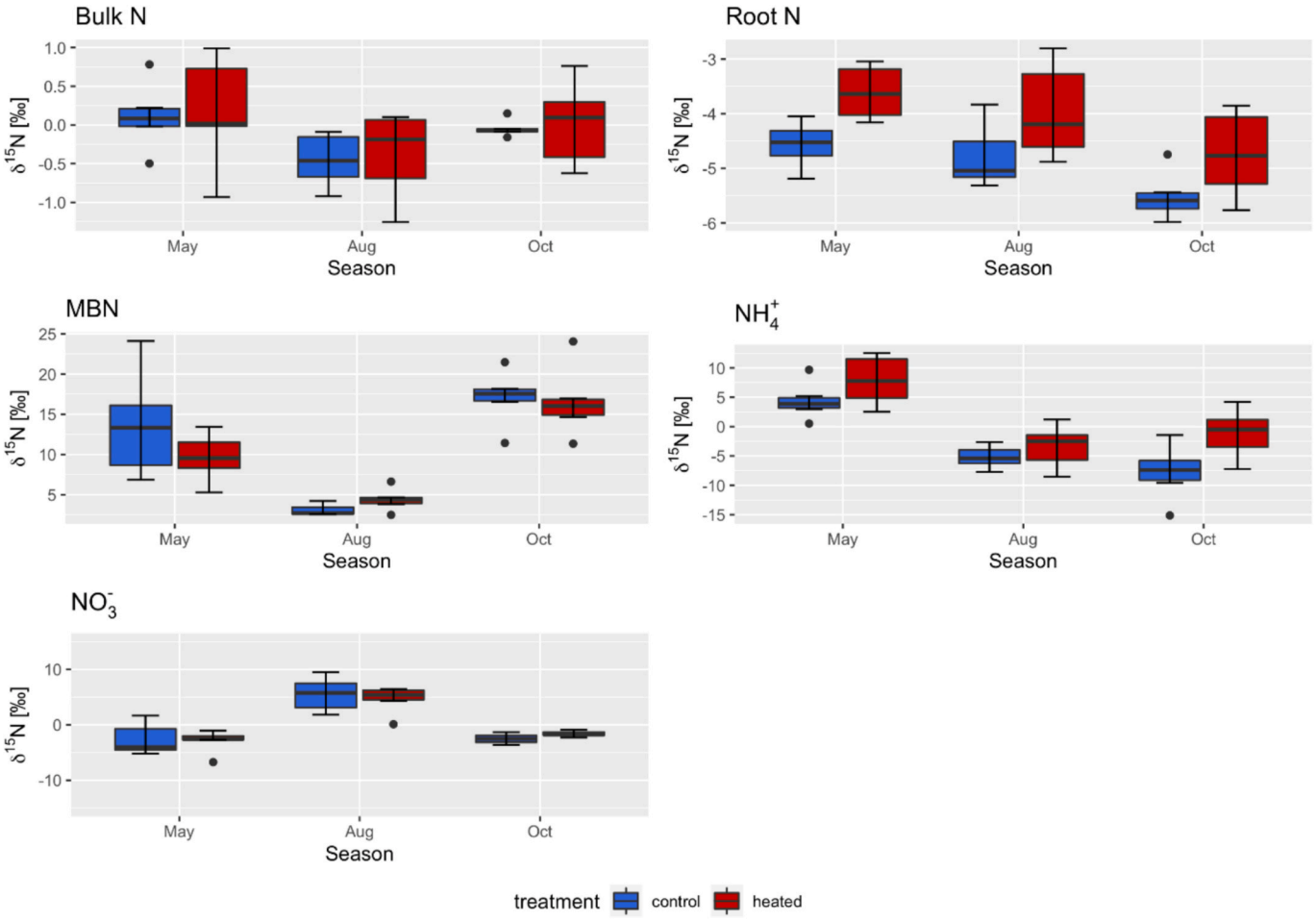

Fig. 2. Isotopic signatures ($\delta^{15}N$ values) of belowground N pools in warmed and control plots in the old-growth forest warming experiment in Achenkirch, Tyrol, Austria, during three sampling seasons.

values of bulk soil and MBN showed a minimum during summer, while $\delta^{15}N$ values of soil NO_3^- peaked during summer, and those of roots and soil NH_4^+ declined across the vegetation season. Soil warming caused ^{15}N enrichment of root N and soil NH_4^+, with $\delta^{15}N$ values of roots ($p < 0.001$) and of soil NH_4^+ ($p = 0.0022$) significantly increasing in warmed soils (Fig. 2, Table 1).

Measured $\delta^{15}N_{NO3}$ values were much higher than expected according to the simple calculation using the isotope effect of nitrification of 29.6‰ according to Denk et al. (2017). Applying the simplified $\delta^{15}N$ model based partitioning approach for NO_3^- sink processes (Equation (4) shows that denitrification contributed more than leaching to soil NO_3^- losses, with fractions of $f_{denitrification}$ of 0.65 in control soils and 0.60 in warmed soils, and this was consistent across seasons. In controls, $f_{denitrification}$ changed from 0.51 in May to 0.67–0.72 in August and October, while in warmed soils the values changed from 0.45 in May to 0.60–0.70 in August and October (Table S1). Given the many uncertainties underlying these calculations (see Materials and Methods and Discussion), we performed the calculations only on mean values and did not perform statistical tests on $f_{denitrification}$.

4. Discussion

In the Achenkirch warming experiment, we expected to find changes in $\delta^{15}N$ signatures of inorganic soil N pools to reflect a warming-induced stimulation of organic N mineralization, nitrification, and NO_3^- loss processes. We further predicted the isotopic alterations to mirror an opening of the ecosystem N cycle with greater N losses in response to soil warming. The results generally showed an increase in nitrification,

causing ^{15}N enrichment of soil NH_4^+, while the partitioning between N loss pathways was not directly affected. However, the stimulation of nitrification caused overall greater soil NO_3^- losses, with denitrification dominating over NO_3^- leaching.

4.1. Warming effects of fine root $\delta^{15}N$ reflect changes in inorganic N

Among the studied soil nitrogen pools, only root N and soil NH_4^+ were significantly altered, showing ^{15}N enrichment in the warming treatment. These two pools are inherently connected as plants and their roots take up soil inorganic N and therefore isotopically mirror underlying (changes in) soil inorganic N transformation processes. NH_4^+ covers a large fraction of plant N demand, particularly in forests, with smaller contributions of organic N and NO_3^- (Hu et al. 2024; Mao et al. 2025a). The increase in fine root $\delta^{15}N$ therefore mirrors the ^{15}N enrichment in soil NH_4^+ and indicates that soil NH_4^+ significantly contributed to root N uptake in this montane forest under warmed conditions. Root NH_4^+ uptake was shown to contribute disproportionately to total N uptake in ectomycorrhizal temperate trees (Liu et al. 2017), such as spruce and beech dominating the Achenkirch forest, while organic N forms and NO_3^- contribute less. Differences in $\delta^{15}N$ values between organic N forms, NH_4^+ and NO_3^- in soils coupled with those in tree biomass have also been applied globally to show that NH_4^+ uptake dominates over NO_3^- and organic N uptake in temperate biomes (Hu et al. 2024).

4.2. Warming causes ^{15}N enrichment of soil ammonium but does not affect MBN

The significant increase in $\delta^{15}N_{NH4+}$ values indicates that experimental warming altered NH_4^+ turnover processes. A recent meta-analysis reported that climate warming stimulates soil N mineralization by 22%, particularly in forests and grasslands (Mao et al. 2025b). Consistent with this, gross N mineralization rates in the Achenkirch forest increased by 63% under warming during the same sampling campaign as in this study (Tian et al. 2023a). Enhanced N mineralization is expected to fractionate N isotopes, producing ^{15}N depleted NH_4^+ while enriching the residual organic N substrate (SON) in ^{15}N. However, because SON constitutes more than 95% of total soil N and turns over slowly, its bulk isotopic composition is unlikely to respond detectably to short-term changes in isotope fractionation processes. The absence of a measurable $\delta^{15}N$ response in bulk soil therefore likely reflects the large size and isotopic inertia of the SON pool rather than lack of isotope fractionation during mineralization.

MBN represents a more dynamic N pool and showed strong ^{15}N enrichment relative to bulk soil N ($\delta^{15}N_{MBN}$ = 3–18‰ vs. − 1 to 1‰). Despite this substantial ^{15}N enrichment, MBN $\delta^{15}N$ did not differ between warmed and control soils. This indicates that microbial biomass did not reflect the warming-induced increase in gross N mineralization observed at the site. Instead, $\delta^{15}N_{MBN}$ exhibited pronounced spatial and seasonal variability, suggesting that microbial N isotope composition is primarily controlled by short-term shifts in microbial N metabolism rather than by warming per se.

Microbial ^{15}N enrichment is expected to increase when organic N uptake exceeds anabolic demand and excess N is excreted as ^{15}N-depleted NH_4^+. This relationship is closely associated with microbial NUE, which has been reported to decrease in earlier studies at Achenkirch, reflecting a shift toward more catabolic nitrogen metabolism and greater NH_4^+ excretion (Shi et al. 2023; Tian et al. 2023b). Qualitatively, such a shift would be consistent with enhanced microbial ^{15}N enrichment. However, the lack of a detectable warming effect on $\delta^{15}N_{MBN}$ suggests that this signal was masked by strong temporal and spatial variability in microbial N dynamics.

Seasonal patterns further support the role of anabolic–catabolic balance in controlling microbial $\delta^{15}N$. In spring and autumn, MBN was low while $\delta^{15}N$ MBN was high, whereas in summer MBN increased and $\delta^{15}N$ MBN declined. These shifts are consistent with periods of enhanced catabolic cycling of organic N, characterized by reduced microbial biomass and increased ^{15}N enrichment due to the excretion of ^{15}N-depleted NH_4^+, versus periods favoring anabolic assimilation of C and N, leading to greater microbial growth and lower $\delta^{15}N_{MBN}$.

Similar relationships between microbial growth state and microbial biomass $\delta^{15}N$ have been observed in bacterial cultures (Collins et al. 2008) and in other soils (Dijkstra et al. 2008; Shinoda et al. 2019). The magnitude of $\delta^{15}N_{MBN}$ enrichment depends on the isotope fractionation associated with organic N mineralization. While this isotope fractionation was previously assumed to be small (~2‰; Högberg 1997), recent field evidence suggests substantially larger effects ($\Delta_{mineralization}$ averaged 12.7‰; Xu et al. 2021). Consequently, NH_4^+ produced during N mineralization is expected to be markedly ^{15}N depleted, consistent with the low $\delta^{15}N_{NH4+}$ values observed in some sampling periods (e.g., −3 to −7‰ in October), although this pattern was not consistent across seasons.

With NH_4^+ subsequently becoming a substrate for nitrification ($\Delta_{nitrification}$ 29.6‰; Denk et al. 2017), the observed greater ^{15}N enrichment of NH_4^+ in warmed soils indicates that a larger fraction of NH_4^+ has been consumed by nitrifiers, meaning that more NO_3^- was formed in warmed soils. While gross nitrification rates in the same soil samples did not respond to warming (Tian et al. 2023a), a meta-analysis demonstrated globally that warming promotes nitrification in soils (Mao et al. 2025b), linked to changes in the abundance of ammonia-oxidizing bacteria and changes in soil moisture. Interestingly, the stimulation of nitrification was linked to wetter conditions, not to drier ones as drier conditions caused smaller stimulations of nitrification (Mao et al. 2025b). We could not link the increase in nitrification to changes in nitrifier abundance. However, temperature and moisture are strongly linked at the soil and ecosystem level, and with continuous soil warming soil moisture declines (Xu et al., 2013). Decreased soil moisture was also found intermittently in Achenkirch during rain-free periods, though high MAP and frequent precipitation events regularly reset these differences. However, under wet conditions small decreases in soil moisture can improve soil oxygenation and general organic matter decomposition, both stimulating nitrifiers by alleviating substrate (O_2, NH_4^+) limitation.

The interpretation of warming-responses of nitrification based on $\delta^{15}N$ data can contradict the direct measurements of gross nitrification made on the same soils for two reasons: (i) Natural-abundance $\delta^{15}N$ patterns reflect changes in flux partitioning within the soil N cycle, whereas isotope pool dilution measurements isolate gross process rates over short incubations and test whether a single process changes in absolute terms. Enrichment of the NH_4^+ pool indicates that a larger fraction of mineralized NH_4^+ was consumed by nitrification; however, proportional changes in N mineralization and nitrification would not alter this fractional consumption and thus would not be expressed in $\delta^{15}N$ changes. In addition, (ii) gross rates integrate processes over a few hours, while $\delta^{15}N$ integrates over the longer turnover times of NH_4^+ and NO_3^- pools, so that the two approaches capture different temporal horizons and need not converge quantitatively.

4.3. Partitioning nitrate losses to leaching and denitrification, and its uncertainties

Faster N mineralization and nitrification stimulate NO_3^- formation in warmed soils, potentially fueling N loss processes. Losses of ^{15}N-depleted N forms, such as NO_3^- via leaching or gaseous N species produced during denitrification, result in progressive ^{15}N enrichment of residual ecosystem N pools, but as proposed in this study, hydrological and gaseous NO_3^- loss pathways can be distinguished by their differential isotope effects on residual nitrate.

Although nitrate production rates increased under soil warming, neither the isotopic composition of soil NO_3^- nor the inferred relative contributions of nitrate loss pathways differed significantly between warmed and control soils. Based on the isotope model, denitrification

accounted for the dominant fraction of soil NO_3^- losses, with estimated $f_{denitrification}$ values averaging ~ 60% in warmed soils and ~ 65% in control soils. However, these estimates must be interpreted with considerable caution requiring consideration of three main factors causing uncertainty in our N loss estimates: (i) divergence of isotope discrimination values of nitrification and denitrification from literature means, (ii) occurence of other NO_3^- source or sink processes, and (iii) external nitrate input by atmospheric deposition.

(i) Isotope discrimination values for nitrification and denitrification are primarily derived from microbial isolates and a limited number of complex soil communities (Denk et al. 2017). In soils, isotope effects are typically "apparent" rather than intrinsic, because diffusion limitation, microbial assimilation, and coupled nitrification–denitrification processes can obscure organism-level isotope fractionation. Consequently, reported apparent isotope effects vary widely, with net nitrification estimates ranging from ~ 7–11‰ to 25–31‰ (Yun and Ro, 2014; Yu et al., 2021). To assess how this uncertainty affects our estimates of denitrification-derived nitrate loss ($f_{denitrification}$) we performed a sensitivity analysis in which isotope discrimination values of nitrification and/or denitrification were reduced by half (from ~ 30‰ to ~ 15‰; Table S1). Lower $\Delta_{nitrification}$ reduced $f_{denitrification}$ to 0.35 (control) and 0.43 (warmed), whereas lower $\Delta_{denitrification}$ increased $f_{denitrification}$ to 0.88 and 0.84, respectively. When both isotope effects were reduced simultaneously, $f_{denitrification}$ remained similar to the original estimates (0.68 and 0.58). Overall, uncertainty in isotope fractionation can shift $f_{denitrification}$ by ~ 20%. However, the relative comparison between warmed and control soils was robust to these changes. Better constraints on intrinsic isotope effects in soils would nevertheless improve confidence in quantitative N loss partitioning.

(ii) Additional nitrate-consuming processes may influence isotopic signals. Besides denitrification, dissimilatory nitrate reduction to ammonium (DNRA) converts NO_3^- to NH_4^+ under low O_2 conditions, thus recycling N rather than causing net losses. Because DNRA and denitrifiers use the same enzyme for the first nitrate reduction step and their isotope effects on nitrate are expected to be comparable (Asamoto et al. 2021), DNRA would not alter nitrate isotope enrichment but could lead to overestimation of denitrification-derived N losses. In contrast, microbial and plant NO_3^- assimilation exhibit much smaller isotope fractionation under field conditions (Evans 2001; Denk et al. 2017). If substantial, these processes would reduce the apparent isotope enrichment of residual NO_3^- and thus lower estimated $f_{denitrification}$. Improved constraints on the rates and isotope effects of these processes would therefore refine model-based estimates of nitrate loss pathways.

(iii) Atmospheric deposition of reactive N (NH_4^+ and NO_3^-) can introduce isotopically distinct NO_3^- to soil pools, potentially affecting isotope-based estimates of nitrate loss pathways. At the study site, total N deposition (~18 kg N ha^{-1} yr^{-1}) is comparable in magnitude to annual NO_3^- leaching losses (7–12 kg N ha^{-1} yr^{-1}; Kalina et al 2002; this study). However, deposited NO_3^- is ^{15}N-depleted (−7 to 6‰, mean − 3‰; Haberhauer et al. 2002) and would therefore dilute, rather than enhance, the ^{15}N enrichment of soil nitrate. As a result, atmospheric N inputs would lead to underestimating $f_{denitrification}$. Explicitly accounting for N deposition in an isotope mass balance would require well-constrained internal soil N fluxes, particularly gross mineralization and nitrification, which are highly uncertain and substantially larger than external inputs. For example, gross nitrification at the site produces ~ 190 kg NO_3^-–N ha^{-1} yr^{-1} (Tian et al. 2023a), exceeding atmospheric nitrate inputs by more than an order of magnitude. We therefore retained a simplified isotope-based partitioning approach and acknowledge the associated uncertainties.

Despite these limitations, natural abundance ^{15}N approaches offer a valuable and complementary perspective on ecosystem N cycling. Unlike direct flux measurements, which provide instantaneous rates (e.g. kg N ha^{-1} yr^{-1} or mg N kg^{-1} d^{-1}), isotope-based analyses integrate processes over longer time scales related to N residence times in soil and plant pools. Importantly, this information is obtained non-invasively from *in situ* sampling, without tracer additions or experimental disturbance, and thus reflects the cumulative imprint of microbial processing, retention, and loss pathways. When interpreted cautiously and in conjunction with independent flux measurements, stable isotope data provide unique insight into the partitioning and long-term regulation of ecosystem N losses under climate change.

5. Conclusion

In this study we revealed two main outcomes related to soil warming effects on soil N flux partitioning, thus affecting the isotope fingerprints of different nitrogen pools. (i) Nitrification was accelerated in warmed soils causing a larger fraction of NH_4^+ being converted to nitrate and increased ^{15}N enrichment of soil NH_4^+. Elevated nitrification is directly linked to an increased risk of N losses through NO_3^- leaching and denitrification. Denitrification dominated NO_3^- losses but the share of NO_3^- losses attributed to denitrification was not affected by warming. (ii) The isotopic characterization of residual substrates of N processes such as NH_4^+ for nitrification and NO_3^- for leaching and denitrification allows alternative determinations of changes in the N flux balance in response to global change factors. Time integrated fluxes are hard to quantify *in situ* using ^{15}N tracing of gross process rates and gas flux measurements, including NO, N_2O and N_2 to fully quantify mineralization, nitrification and denitrification activity. A $\delta^{15}N$ model based partitioning approach therefore allows non-invasive complementary insights into the intricate complexities of the terrestrial N cycle and its environmental sensitivity. Integrating isotopic approaches into long-term monitoring can support the prediction of nitrogen loss risks, especially under climate warming. Furthermore, such functional indicators can improve the accuracy of nutrient cycle models under future climate scenarios.

CRediT authorship contribution statement

Michaela Bachmann: Writing – review & editing, Writing – original draft, Visualization, Validation, Investigation, Formal analysis, Data curation, Conceptualization. **Ye Tian:** Writing – review & editing, Investigation. **Jakob Heinzle:** Investigation. **Werner Borken:** Writing – review & editing. **Erich Inselsbacher:** Writing – review & editing. **Wolfgang Wanek:** Writing – review & editing, Writing – original draft, Validation, Investigation, Formal analysis, Conceptualization. **Andreas Schindlbacher:** Writing – review & editing, Project administration.

Declaration of competing interest

The authors declare that they have no known competing financial interests or personal relationships that could have appeared to influence the work reported in this paper.

Acknowledgements

We would like to thank Margarete Watzka, Ludwig Seidl and Sabrina Pober for technical support in the laboratory and Michael Gasser for support with the graphical abstract.

We also thank our three reviewers for their significant feedback and input.

Declaration of generative AI and AI-assisted technologies in the manuscript preparation process

During the preparation of this work the author(s) used ChatGTP in order to improve readability and language. After using this tool/service, the author(s) reviewed and edited the content as needed and take(s) full responsibility for the content of the published article.

Appendix A. Supplementary data

Supplementary data to this article can be found online at https://doi.org/10.1016/j.geoderma.2026.117746.

Data availability

Data will be made available on request.

References

Asamoto, C.K., Rempfert, K.R., Luu, V.H., Younkin, A.D., Kopf, S.H., 2021. Enzyme-specific Coupling of Oxygen and Nitrogen Isotope Fractionation of the Nap and Nar Nitrate Reductases. Environ. Sci. Technol. 55 (8), 5537–5546. https://doi.org/10.1021/acs.est.0c07816.

Bai, E., Li, S., Xu, W., Li, W., Dai, W., Jiang, P., 2013. A Meta-Analysis of Experimental Warming Effects on Terrestrial Nitrogen Pools and Dynamics. New Phytol. 199 (2), 441–451. https://doi.org/10.1111/nph.12252.

Bates, D., Maechler, M., Bolker, B., Walker, S., 2015. Fitting Linear Mixed-Effects Models using lme4. J. Stat. Softw. 67 (1), 1–48. https://doi.org/10.18637/jss.v067.i01.

Barton, K. 2020. MuMIn: Multi-Model Inference. R package version 1.43.17. https://CRAN.R-project.org/package=MuMIn.

Butler, S.M., Melillo, J.M., Johnson, J.E., Mohan, J., Steudler, P.A., Lux, H., Burrows, E., Smith, R.M., Vario, C.L., Scott, L., Hill, T.D., Aponte, N., Bowles, F., 2012. Soil Warming Alters Nitrogen Cycling in a New England Forest: Implications for Ecosystem Function and Structure. Oecologia 168 (3), 819–828. https://doi.org/10.1007/s00442-011-2133-7.

Canadell, J.G., Meyer, C.P., Cook, G.D., Dowdy, A., Briggs, P.R., Knauer, J., Pepler, A., Haverd, V., 2021. Multi-Decadal increase of Forest burned Area in Australia is Linked to climate Change. Nat. Commun. 12 (1), 6921. https://doi.org/10.1038/s41467-021-27225-4.

Collins, J.G., Roe, S.M., Bracht, J., 2008. Nitrogen source influences natural abundance 15 N of *Escherichia coli*. FEMS Microbiol. Lett. 282 (2), 246–250. https://doi.org/10.1111/j.1574-6968.2008.01133.x.

Dawes, M.A., Schleppi, P., Hättenschwiler, S., Rixen, C., Hagedorn, F., 2017. Soil warming opens the nitrogen cycle at the alpine treeline. Glob. Chang. Biol. 23, 421–434.

Dawson, T.E., Siegwolf, R.T.W., 2007. Using Stable Isotopes as Indicators, Tracers, and Recorders of Ecological Change: some Context and Background. In: Dawson, T.E., Siegwolf, R.T.W. (Eds.), Stable Isotopes as Indicators of Ecological Change. Elsevier, pp. 3–18.

Denk, T. R., Mohn, J., Decock, C., Lewicka-Szczebak, D., Harris, E., Butterbach-Bahl, Kiese, R. & B. Wolf. 2017. The nitrogen cycle: A review of isotope effects and isotope modeling approaches. Soil Biology and Biochemistry 105, 121-137.

Dijkstra, P., LaViolette, C.M., Coyle, J.S., Doucett, R.R., Schwartz, E., Hart, S.C., Hungate, B.A., 2008. ^{15}N enrichment as an integrator of the effects of C and N on microbial metabolism and ecosystem function. Ecol. Lett. 11 (4), 389–397. https://doi.org/10.1111/j.1461-0248.2008.01154.x.

Evans, R.D., 2001. Physiological Mechanisms Influencing Plant Nitrogen Isotope Composition. Trends Plant Sci. 6 (3), 121–126. https://doi.org/10.1016/S1360-1385(01)01889-1.

Haberhauer, G., Gerzabek, M.H., Krenn, A., 2002. Nitrate dynamics in an Alpine forest site (Mühleggerköpfl). O and N stable isotope analysis in natural water samples. Environmental Science and Pollution Research (special Issue), Spec No 2, 37–41. https://doi.org/10.1007/BF02987476.

Handley, L.L., Raven, J.A., 1992. The use of natural abundance of nitrogen isotopes in plant physiology and ecology. Plant Cell Environ. 15 (9), 965–985.

Heinzle, J., Wanek, W., Tian, Y., Kengdo, S.K., Borken, W., Schindlbacher, A., Inselsbacher, E., 2021. No effect of long-term soil warming on diffusive soil inorganic and organic nitrogen fluxes in a temperate forest soil. Soil Biol. Biochem. 158, 108261.

Heinzle, J., Kitzler, B., Zechmeister-Boltenstern, S., Tian, Y., Kwatcho Kengdo, S., Wanek, W., Borken, W., Schindlbacher, A., 2023. Soil CH_4 and N_2O response diminishes during decadal soil warming in a temperate mountain forest. Agric. For. Meteorol. 329, 109287. https://doi.org/10.1016/j.agrformet.2022.109287.

Högberg, P. 1997. Tansley review no. 95: ^{15}N natural abundance in soil–plant systems. *The New Phytologist 137,* no. 2: 179-203.

Hu, C.-C., Liu, X.-Y., Driscoll, A.W., Kuang, Y.-W., Brookshire, E.N.J., Lü, X.-T., Chen, C.-J., Song, W., Mao, R., Liu, C.-Q., Houlton, B.Z., 2024. Global distribution and Drivers of Relative Contributions among Soil Nitrogen sources to Terrestrial Plants. Nat. Commun. 15, 6407. https://doi.org/10.1038/s41467-024-50674-6.

IUSS Working Group WRB. 2022. World Reference Base for Soil Resources. International soil classification system for naming soils and creating legends for soil maps. 4th edition. International Union of Soil Sciences (IUSS), Vienna, Austria. https://www.isric.org/sites/default/files/WRB_fourth_edition_2022-12-18.pdf. Last accessed 11.08.2025.

Jenkinson, D.S., Brookes, P.C., Powlson, D.S., 2004. Measuring soil microbial biomass. Soil Biol. Biochem. 36 (1), 5–7. https://doi.org/10.1016/j.soilbio.2003.10.002.

Kalina, M. F., S. Stopper, E. Zambo, and H. Puxbaum. 2002. Altitude-dependent Wet, Dry and Occult Nitrogen Deposition in an Alpine Region. Environmental Science and Pollution Research 9 (Special Issue 2): 16–22. https://doi.org/10.1007/BF02987473.

Kuznetsova, A., Brockhoff, P.B., Christensen, R.H.B., 2017. lmerTest Package: Tests in Linear mixed Effects Models. J. Stat. Softw. 82 (13), 1–26.

Lachouani, P., Frank, A.H., Wanek, W., 2010. A suite of sensitive chemical methods to determine the δ15N of ammonium, nitrate and total dissolved N in soil extracts. Rapid Commun. Mass Spectrom. 24 (24), 3615–3623.

Liao, K., Lai, X., Zhu, Q., 2021. Soil $\delta^{15}N$ is a better indicator of ecosystem nitrogen cycling than plant $\delta^{15}N$: a global meta-analysis. Soil 7 (733–742), 2021. https://doi.org/10.5194/soil-7-733-2021.

Liu, M., Li, C., Xu, X., Wanek, W., Jiang, N., Wang, H., Yang, X., 2017. Organic and inorganic nitrogen uptake by 21 dominant tree species in temperate and tropical forests. Tree Physiol. 37 (11), 1515–1526. https://doi.org/10.1093/treephys/tpx046.

Mao, J., Wang, J., Liao, J., Xu, X., Tian, D., Zhang, R., Peng, J., Niu, S., 2025. *Plant nitrogen uptake preference and drivers in natural ecosystems at the global scale.* New Phytol. 246 (3), 972–983. https://doi.org/10.1111/nph.70030.

Mao, C., Wang, Y., Ran, J., Wang, C., Yang, Z., Yang, Y., 2025. Effects of warming and precipitation change on soil nitrogen cycles: a meta-analysis [Article] J. Plant Ecol. 18 (3). https://doi.org/10.1093/jpe/rtaf051.

Mariotti, A., Germon, J.C., Hubert, P., Kaiser, P., Letolle, R., Tardieux, A., Tardieux, P., 1981. Experimental determination of nitrogen kinetic isotope fractionation: some principles; illustration for the denitrification and nitrification processes. Plant and Soil 62 (3), 413–430.

Meng, C., Tian, D., Zeng, H., Li, Z., Chen, H.Y.H., Niu, S., 2020. *Global meta-analysis on the responses of soil extracellular enzyme activities to warming.* Sci. Total Environ. 705, 135992. https://doi.org/10.1016/j.scitotenv.2019.135992.

Nolan, C., Overpeck, J.T., Allen, J.R.M., Anderson, P.M., Betancourt, J.L., Binney, H.A., et al., 2018. Past and Future Global Transformation of Terrestrial Ecosystems under climate Change. Science 361 (6405), 920–993. https://doi.org/10.1126/science.aan5360.

Pinheiro, J., Bates, D., DebRoy, S., Sarkar, D. & R Core Team. 2019. nlme: Linear and Nonlinear Mixed EffectsModels. R package version 3.1-143.

Salazar, A., Magnusson, C., Jonsdottir, A.S., Hansen, G.M., Stevenson, C.R., Olofsson, E. G., McGuire, S.D., 2020. Faster Nitrogen Cycling and more Fungal and root Biomass in Cold Ecosystems under Experimental Warming: a Meta-Analysis. Ecology 101 (2), e02938. https://doi.org/10.1002/ecy.2938.

Schindlbacher, A., Schnecker, J., Takriti, M., Borken, W., Wanek, W., 2015. Microbial physiology and soil CO2 efflux after 9 years of soil warming in a temperate forest–no indications for thermal adaptations. Glob. Chang. Biol. 21 (11), 4265–4277.

Shi, C., Urbina-Malo, C., Tian, Y., Heinzle, J., Kwatcho Kengdo, S., Inselsbacher, E., Borken, W., Schindlbacher, A., Wanek, W., 2023. Does long-term soil warming affect microbial element limitation? a test by short-term assays of microbial growth responses to labile C, N and P additions. Glob. Chang. Biol. 29 (8), 2188–2202. https://doi.org/10.1111/gcb.16591.

Shinoda, K., Yano, M., Yoh, M., Yoshida, M., Makabe, A., Yamagata, Y., Houlton, B.Z., Koba, K., 2019. Control of the nitrogen isotope composition of the fungal biomass: evidence of microbial nitrogen use efficiency. Microbes Environ. 34 (1), 5–12. https://doi.org/10.1264/jsme2.ME18082.

Sun, Y., Wang, C., Chen, H.Y.H., Liu, Q., Ge, B., Tang, B., 2022. A Global Meta-Analysis on the responses of C and N Concentrations to Warming in Terrestrial Ecosystems. Catena 208, 105762. https://doi.org/10.1016/j.catena.2021.105762.

Tian, Y., Schindlbacher, A., Urbina Malo, C., Shi, C., Heinzle, J., Kwatcho Kengdo, S., Inselsbacher, E., Borken, W., Wanek, W., 2023. Long-term warming of a forest soil reduces microbial biomass and its carbon and nitrogen use efficiencies. Soil Biol. Biochem. 184, 109109. https://doi.org/10.1016/j.soilbio.2023.109109.

Tian, Y., Shi, C., Urbina Malo, C., Kwatcho Kengdo, S., Heinzle, J., Inselsbacher, E., Ottner, F., Borken, W., Michel, K., Schindlbacher, A., Wanek, W., 2023. Long-term soil warming decreases microbial phosphorus utilization by increasing abiotic phosphorus sorption and phosphorus losses. Article 864 Nat. Commun. 14 (1). https://doi.org/10.1038/s41467-023-36527-8.

Wang, L., 2024. Global Plant Nitrogen Use is Controlled by Temperature. Nat. Commun. 15, 7651. https://doi.org/10.1038/s41467-024-50803-1.

Wickham, H., 2016. ggplot2: Elegant Graphics for Data Analysis. Springer-Verlag, New York.

Xu, W., Yuan, W., Dong, W., Xia, J., Liu, D., Chen, Y., 2013. A meta-analysis of the response of soil moisture to experimental warming. Environ. Res. Lett. 8 (4), 044027.

Xu, S.Q., Liu, X.Y., Sun, Z.C., Hu, C.C., Wanek, W., Koba, K., 2021. Isotopic elucidation of microbial nitrogen transformations in forest soils. Global Biogeochem. Cycles 35, no. 12. https://doi.org/10.1029/2021GB007070.

Yu, L., Zheng, T., Hao, Y., Zheng, X., 2021. Determination of the Nitrogen Isotope Enrichment factor Associated with Ammonification and Nitrification in Unsaturated Soil at Different Temperatures. Environ. Res. 202, 111670. https://doi.org/10.1016/j.envres.2021.111670.

Yuan, Y., Ge, L., Yang, H., Ren, W., 2018. A Meta-Analysis of Experimental Warming Effects on Woody Plant Growth and Photosynthesis in Forests. J. For. Res. 29 (3), 727–733. https://doi.org/10.1007/s11676-017-0499-z.

Yun, S.-I., Ro, H.-M., 2014. Can Nitrogen Isotope Fractionation Reveal Ammonia Oxidation responses to Varying Soil Moisture? Soil Biol. Biochem. 76, 136–139. https://doi.org/10.1016/j.soilbio.2014.04.032.

Zhang, S., Fang, Y., Xi, D., 2015. Adaptation of micro-diffusion method for the analysis of ^{15}N natural abundance of ammonium in samples with small volume. Rapid Commun. Mass Spectrom. 29 (14), 1297–1306. https://doi.org/10.1002/rcm.7224.